2003

Modeling Heat Conduction in Spiral Geometries

Parthasarathy M. Gomadam
University of South Carolina - Columbia

Ralph E. White
University of South Carolina - Columbia, white@cec.sc.edu

John W. Weidner
University of South Carolina - Columbia, weidner@engr.sc.edu

Publication Info

Journal of the Electrochemical Society, 2003, pages A1339-A1345.

Publisher's link: http://dx.doi.org/10.1149/1.1605743
DOI: 10.1149/1.1605743

Journal of The Electrochemical Society, **150** (10) A1339-A1345 (2003)
0013-4651/2003/150(10)/A1339/7/$7.00 © The Electrochemical Society, Inc.

Modeling Heat Conduction in Spiral Geometries

Parthasarathy M. Gomadam,* Ralph E. White, and John W. Weidner***,z**

Center for Electrochemical Engineering, Department of Chemical Engineering, University of South Carolina, Columbia, South Carolina 29208, USA

A two-dimensional (2-D) energy balance (the 2D model) is reduced to a one-dimensioanl (1-D) energy balance (the 1D-radial-spiral model) by a coordinate transformation approach. The 1D-radial-spiral model, even though 1-D, captures both radial and spiral heat conductions over a wide range of design parameters. By comparing the temperature predictions of the 1D-radial-spiral model and the 2D model, parameter ranges were identified where spiral conduction was important and where the 1D-radial-spiral model held. The 1D-radial-spiral model provided a sixtyfold savings in computation time over the 2D model. When coupled to electrochemistry, the 2D model took approximately 20 h to simulate a 2C discharge of a Li-ion battery, while the 1D-radial-spiral model took about 20 min.
 [DOI: 10.1149/1.1605743]

Manuscript submitted September 10, 2002; revised manuscript received April 25, 2003. Available electronically August 25, 2003.

The spirally wound design is of importance to battery manufacturers as it improves the energy and power densities, by using lesser accessories when compared with the prismatic design.[1-2] For this reason, the spirally-wound design is used in a variety of battery systems (*e.g.*, Li-$SOCl_2$,[3] Li bromine chloride complexing additive (BCX),[4] lead-acid,[5] Zn-MnO_2,[6] Li-ion[1-2,7]). However, because of their lower surface area to volume ratio, spiral batteries retain more heat than prismatic batteries. Therefore, in order to improve thermal management and achieve safe operation of large-scale spirally wound batteries, it is important to understand their thermal behavior, especially during high rate operation.

A cost effective method of studying heat transport during the operation of a battery is to theoretically simulate the temperatures attained by the battery. However, very few publications[3-9] exist in the literature that couple electrochemical and thermal behavior in spirally wound batteries. Rather, most thermal models of spirally wound batteries estimate the heat generation rate *a priori* from experimental voltage-time data.[3-4,7-9] Cho and Halpert[8] and Cho[9] assumed that the entire battery operates at a uniform temperature, while Al Hallaj *et al.*[7] simulated a 1-D radial variation in temperature. Evans and White[3] and Kalu and White[4] accounted for both radial and spiral heat conductions in their spirally wound battery systems using a two-dimensional (2-D) model for the energy balance. Evans and White[3] compared the predictions of the 2-D model with a 1-D model that considers only radial heat conduction, and showed that the latter model significantly overpredicted temperature. Evans and White[3] also presented a lumped form of the 1-D model by averaging the thermal properties of the battery. This model was shown to underpredict the center temperature in comparison with the 2-D model. Thus, they concluded that in order to predict the thermal behavior of their spirally wound batteries, the energy balance equation must be solved in two dimensions. Harb and LaFollette[5] followed the two-dimensional approach of Evans and White[3] to study the thermal behavior of a spirally wound lead-acid battery. However, they calculated the heat generation rate theoretically by coupling the thermal model to an electrochemical model. As argued by Rao and Newman,[10] coupling electrochemical and thermal behavior is critical in calculating temperatures accurately.

Solving a 2-D coupled electrochemical-thermal model, however, is computationally a very demanding task. For example, Harb and LaFollette[5] report that for simulating a 10C discharge (from 100-50% state-of-charge) of their spirally wound lead-acid battery approximately 70 h of solution time was required. Similarly, in simulating a typical discharge of a prismatic Li-ion battery using a 2-D electrochemical-thermal model, Song and Evans[11] reported a solution time of several days. Therefore, to reduce the solution time, efficient algorithms and solution techniques are being developed by researchers.[12] A complementary approach would be to attempt a simplification of the problem (*i.e.*, the governing differential equation) itself, as is done here for spirally wound batteries.

This paper presents the derivation of the 2-D energy balance equation (the 2D model) for heat conduction in a spiral made of two materials having different thermal properties. By using average values for the radial and spiral thermal conductivities in the 2D model, we reduced it to a 1-D model (the 1D-radial-spiral model) through a coordinate-transformation technique. The 1D-radial-spiral model, even though 1-D, captured both radial and spiral heat conductions. On the other hand, by ignoring the spiral heat conduction term in the 2D model, we derived another 1-D model (the 1D-radial model), which considers only radial heat conduction. We compare the three models over a wide range of design parameters and identify parameter spaces where spiral heat conduction is important and where the 1D-radial-spiral model captures this mode of heat transport.

Model Development

General energy balance (the 2D model).—Consider two plane sheets (S_1 and S_2) of thicknesses (X_1 and X_2) and thermal conductivities (λ_1 and λ_2) rolled into a spiral such that its cross section perpendicular to the axis of rotation looks like that shown in Fig. 1. The differential equation governing temperature in each region of the spiral composite is given by

$$\rho C_p \frac{\partial T}{\partial t} = \nabla(\lambda \nabla T) + \dot{q} \qquad [1]$$

The boundary, interface, and initial conditions are given as

$$\text{at the inner boundary} \quad -\lambda \nabla T = 0 \qquad [2]$$

$$\text{at the outer boundary} \quad -\lambda \nabla T = h(T - T_{amb}) \qquad [3]$$

$$\text{at the interfaces} \quad (-\lambda \nabla T)\big|_{S_1} = (-\lambda \nabla T)\big|_{S_2} \qquad [4]$$

$$\text{at } t = 0 \quad T = T_0 \qquad [5]$$

where

$$\lambda = \begin{cases} \lambda_1 & \text{in } S_1 \\ \lambda_2 & \text{in } S_2 \end{cases} \quad \text{and} \quad \rho C_p = \begin{cases} \rho C_p|_1 & \text{in } S_1 \\ \rho C_p|_2 & \text{in } S_2 \end{cases} \qquad [6]$$

The boundary conditions imply that the core of the spiral is adiabatic, while the outer boundary exchanges heat with the ambience through a heat-transfer coefficient. At the interfaces, the normal heat fluxes were matched, and the spiral was set at a uniform initial temperature of T_0.

* Electrochemical Society Student Member.
** Electrochemical Society Fellow.
*** Electrochemical Society Active Member.
z E-mail: weidner@engr.sc.edu

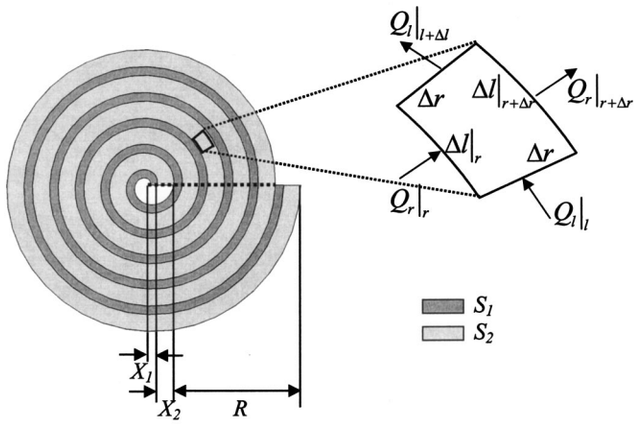

Figure 1. A cross section of the solid composite spiral obtained by rolling two sheets S_1 and S_2 of thicknesses X_1 and X_2. The ring thickness of the spiral is defined as $R \equiv N(X_1 + X_2)$. The fluxes, entering and leaving an arbitrarily chosen surface element are used in Eq. 21 to derive the 2-D energy balance. The dotted line shows the radius chosen in the 1D-radial and the 1D-radial-spiral models.

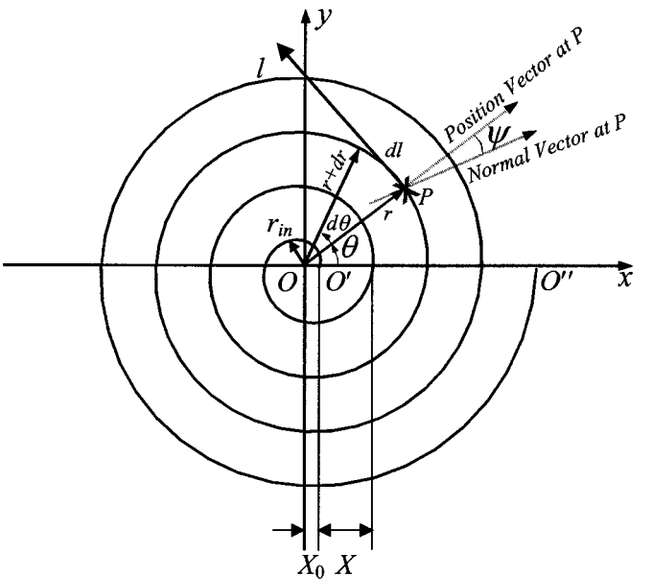

Figure 2. The locus of a point P moving such that $(r\text{-}X_0) \propto \theta$, where r is its distance from the origin O, θ is its angular coordinate, and X_0 is the distance of the starting point O′ from O.

Purely radial heat conduction (the 1D-radial model).—If spiral heat conduction is negligible, Eq. 1 reduces to a 1-D problem given by

$$\rho C_p \frac{\partial T}{\partial t} = \frac{1}{r}\frac{\partial}{\partial r}\left(\lambda r \frac{\partial T}{\partial r}\right) + \dot{q} \qquad [7]$$

This is the governing equation describing radial heat conduction, which, as was also considered by Evans and White,[3] can be solved in two ways as: (i) in which λ is different in each region as given by Eq. 6; (ii) in which λ is uniform and equal to an average over the whole geometry. The first method is a multiregion problem resulting in a step-like radial temperature profile while the second is a single region problem resulting in a smooth temperature profile. Since the first method is more accurate, we use this method for comparing the 1D-radial model results to those from the 1D-radial-spiral model and the 2D model.

The boundary, interface, and initial conditions in the 1D-radial model are given by

$$\text{at } r = r_{in} \quad -\lambda \frac{\partial T}{\partial r} = 0 \qquad [8]$$

$$\text{at } r = (r_{in} + R) \quad -\lambda \frac{\partial T}{\partial r} = h'(T - T_{amb}) \qquad [9]$$

$$\text{at the interfaces } \left(-\lambda \frac{\partial T}{\partial r}\right)\bigg|_{S_1} = \left(-\lambda \frac{\partial T}{\partial r}\right)\bigg|_{S_2} \qquad [10]$$

$$\text{at } t = 0 \quad T = T_0 \qquad [11]$$

As in the 2-D model, here too the boundary conditions (*i.e.*, Eq. 8-9) imply that the core of the spiral was adiabatic and the outer boundary exchanged heat with the ambience. The values of r at the inner and outer boundaries depended on which radius was considered, and is given by

$$r_{in} = r_0 + \frac{\phi}{a} \qquad [12]$$

where

$$a = \frac{2\pi}{X_1 + X_2} \qquad [13]$$

and ϕ is the angle made by any radius of the spiral with the dotted line shown in Fig. 1. However, as is shown later, the temperature distribution in the spiral showed a weak dependence on the angular coordinate. Consequently, one can pick any radius and predict the temperature distribution inside the spiral adequately. For the results shown, the radius given by $\phi = 0$ and $r_{in} = 0$ (*i.e.*, the dotted line itself) was chosen. The variable, R, in Eq. 9 denotes the ring thickness of the spiral as also shown in Fig. 1. Thus, for a spiral of N winds

$$R = N(X_1 + X_2) \qquad [14]$$

The heat-transfer coefficient (h') appearing in Eq. 9 is different from Eq. 3 because the surface area to volume ratio (A/V) of the circular geometry was slightly different from that of the spiral. For the radius, $\phi = 0$, chosen in the 1D-radial model, this quantity was equal to $(2/R)$, while for the spiral, it was $(2/R)[(2N + 1)/2(N + 1)]$. Thus

$$h' = h\frac{(A/V)_{spiral}}{(A/V)_{circular}} = h\left[\frac{2N + 1}{2(N + 1)}\right] \qquad [15]$$

The 1D-radial-spiral model.—When spiral heat conduction was significant, the 1D-radial model did not hold. In contrast, the 1D-radial-spiral model developed in the following paragraphs captures both radial and spiral heat conductions and, therefore, held when spiral conduction was significant. This was achieved by modifying the thermal conductivity (λ) appearing in Eq. 7 so as to include spiral heat conduction. Using the modified thermal conductivity allowed us to capture both radial and spiral heat conductions, while retaining the simplicity of Eq. 7.

In order to modify the thermal conductivity to include spiral heat conduction, we set out deriving the locus of a point moving along a spiral path. The theory developed here is restricted to only one particular kind of spiral, called the Archimedes's spiral. All spiral geometries obtained by rolling sheets with each of which having a uniform thickness fall under this category. For an Archimedes's spiral the deviation of the point from a circular path through its starting point is always proportional to its angular coordinate, θ. Thus, from Fig. 2, $(r - X_0)$ was always proportional to θ. Using the fact that

after one full revolution (*i.e.*, at $\theta = 2\pi$) the distance along the x axis had increased by x, the equation of the spiral was obtained as

$$r = X_0 + \frac{X}{2\pi}\theta \qquad [16]$$

In Cartesian coordinates, the equation of the spiral is expressed in parametric form as

$$x = r\cos\theta \quad \text{and} \quad y = r\sin\theta \qquad [17]$$

with r given by Eq. 16. The differential length (dl) traveled by the point along the spiral was obtained from Fig. 1 as

$$dl^2 = dr^2 + (r\ d\theta)^2 \qquad [18]$$

Eliminating θ between Eq. 16 and 18, we obtained

$$\frac{dl}{dr} = \sqrt{1 + \frac{4\pi^2}{X^2}r^2} \qquad [19]$$

For the spiral composite considered in Fig. 1, this became

$$\frac{dl}{dr} = \sqrt{1 + a^2r^2} \qquad [20]$$

with a given by Eq. 13. This relation is used in decoupling the angular coordinate θ from Eq. 1 to obtain a 1-D partial differential equation governing heat conduction in the spiral composite.

For an arbitrarily chosen surface element of the composite (see Fig. 1), applying energy balance[13] yields

$$\rho C_p\frac{\Delta T}{\Delta t} = \frac{(Q_r\Delta l)|_r - (Q_r\Delta l)|_{r+\Delta r}}{\Delta l\Delta r} + \frac{Q_l|_l - Q_l|_{l+\Delta l}}{\Delta l} + \dot{q} \qquad [21]$$

where

$$Q_r = -\lambda\frac{\partial T}{\partial r} \qquad [22]$$

and

$$Q_l = -\lambda\frac{\partial T}{\partial l} \qquad [23]$$

are the heat fluxes along the radial and spiral directions, respectively. Allowing Δt, Δr, and Δl to tend to zero in Eq. 21, and rearranging, we obtain

$$\rho C_p\frac{\partial T}{\partial t} = -\frac{1}{dl/dr}\frac{\partial}{\partial r}\left(Q_r\frac{dl}{dr}\right) - \frac{\partial Q_l}{\partial l} + \dot{q} \qquad [24]$$

which, with the use of Eq. 20, 22, and 23, yields the governing equation for the energy balance as

$$\rho C_p\frac{\partial T}{\partial t} = \frac{1}{\sqrt{1 + a^2r^2}}\frac{\partial}{\partial r}\left(\lambda\sqrt{1 + a^2r^2}\frac{\partial T}{\partial r}\right) + \frac{\partial}{\partial l}\left(\lambda\frac{\partial T}{\partial l}\right) + \dot{q} \qquad [25]$$

where the thermal properties are discrete functions of position given by Eq. 6. The first and second terms on the right-hand side of this equation correspond to radial and spiral heat conductions, respectively. Using average values for the product ρC_p, and for the thermal conductivities in the radial and spiral directions, and rewriting the operator $\partial/\partial l$ as $(dr/dl)\partial/\partial r$, we get

$$\rho C_p|_{\text{eff}}\frac{\partial T}{\partial t} = \frac{1}{\sqrt{1 + a^2r^2}}\frac{\partial}{\partial r}\left(\lambda_r\sqrt{1 + a^2r^2}\frac{\partial T}{\partial r}\right) + \frac{dr}{dl}\frac{\partial}{\partial r}\left(\lambda_l\frac{dr}{dl}\frac{\partial T}{\partial r}\right) + \dot{q} \qquad [26]$$

With the use of Eq. 20, this becomes

$$\rho C_p|_{\text{eff}}\frac{\partial T}{\partial t} = \frac{1}{\sqrt{1 + a^2r^2}}\frac{\partial}{\partial r}\left(\lambda_r\sqrt{1 + a^2r^2}\frac{\partial T}{\partial r}\right) + \frac{1}{\sqrt{1 + a^2r^2}}\frac{\partial}{\partial r}\left(\frac{\lambda_l}{\sqrt{1 + a^2r^2}}\frac{\partial T}{\partial r}\right) + \dot{q} \qquad [27]$$

The quantity $\rho C_p|_{\text{eff}}$ is obtained by volume averaging as

$$\rho C_p|_{\text{eff}} = \frac{\rho C_p|_1 A_1 + \rho C_p|_2 A_2}{A_1 + A_2} \qquad [28]$$

where the areas, A_1 and A_2, occupied by the two regions are given by

$$A_1 = N\pi x_1(X_1 + R)$$
$$A_2 = N\pi x_2(2X_1 + X_2 + R) \qquad [29]$$

Further, because $a^2r^2 \gg 1$ except very close to the center, Eq. 27 simplifies to

$$\rho C_p\frac{\partial T}{\partial t} = \frac{1}{r}\frac{\partial}{\partial r}\left(r\lambda_{\text{eff}}\frac{\partial T}{\partial r}\right) + \dot{q} \qquad [30]$$

where the effective thermal conductivity (λ_{eff}) includes both the average radial (λ_r) and spiral (λ_l) thermal conductivities, and is given by

$$\lambda_{\text{eff}} = \lambda_r + \frac{\lambda_l}{a^2r^2} \qquad [31]$$

The importance of spiral heat conduction relative to radial heat conduction is obtained from the ratio of the respective components of the effective thermal conductivity (λ_{eff}). Substituting characteristic values for the parameters involved ($\lambda_r = \lambda_1$, $\lambda_l = \lambda_2$, and $r = R$) we obtain the quantity $1/4\pi^2N^2(\lambda_1/\lambda_2)$, where N is the number of winds in the spiral and λ_1/λ_2 is the ratio of the lower to higher thermal conductivity. The higher the value of $1/4\pi^2N^2(\lambda_1/\lambda_2)$, the greater the importance of spiral heat conduction.

The boundary and initial conditions are written as

$$\text{at } r = r_{\text{in}} \quad -\lambda_{\text{eff}}\frac{\partial T}{\partial r} = 0 \qquad [32]$$

$$\text{at } r = (r_{\text{in}} + R) \quad -\lambda_{\text{eff}}\frac{\partial T}{\partial r} = h'(T - T_{\text{amb}}) \qquad [33]$$

$$\text{at } t = 0 \quad T = T_0 \qquad [34]$$

where again we chose the radius, $\phi = 0$, shown dotted in Fig. 1, and the heat-transfer coefficient (h') is given by Eq. 15. No interfacial conditions were required in this model because the spiral composite was assumed to be a single homogeneous material with average thermal properties.

Because spiral conduction occurs along parallel paths in the two materials, the average spiral thermal conductivity (λ_l) was set equal to the thermal conductivity (λ_2) of the more conductive material (taken to be S_2). Radial conduction, however, occurs across the

materials and, therefore, the average radial thermal conductivity (λ_r) was obtained by integrating the radial parts of Eq. 25 and 26 (*i.e.*, the first terms on the right-hand sides). Equating the integrals under steady-state and a zero heat generation rate, we get

$$\lambda_r = \frac{\ln\left[\dfrac{a(R + r_{in}) + \sqrt{1 + a^2(R + r_{in})^2}}{ar_{in} + \sqrt{1 + a^2 r_{in}^2}}\right]}{\Sigma_{i=1}^{N}\left[\dfrac{1}{\lambda_1}\ln\left(\dfrac{ar_{1B} + \sqrt{1 + a^2 r_{1B}^2}}{ar_{1A} + \sqrt{1 + a^2 r_{1A}^2}}\right) + \dfrac{1}{\lambda_2}\ln\left(\dfrac{ar_{2B} + \sqrt{1 + a^2 r_{2B}^2}}{ar_{2A} + \sqrt{1 + a^2 r_{2A}^2}}\right)\right]} \quad [35]$$

where

$$r_{1A} = r_{in} + (i - 1)(x_1 + x_2) \quad [36]$$

$$r_{1B} = r_{1A} + x_1 \quad [37]$$

$$r_{2A} = r_{1B} \quad [38]$$

$$r_{2B} = r_{1B} + x_2 \quad [39]$$

Applying the approximation that $a^2r^2 \gg 1$ in Eq. 35 reduces it to the expression

$$\lambda_r = \frac{\ln\left(\dfrac{R + r_{in}}{r_{in}}\right)}{\Sigma_{i=1}^{N}\left[\dfrac{1}{\lambda_1}\ln\left(\dfrac{r_{1B}}{r_{1A}}\right) + \dfrac{1}{\lambda_2}\ln\left(\dfrac{r_{2B}}{r_{2A}}\right)\right]} \quad [40]$$

which is also given in Ref. 13 for concentric cylinders. However, as the inner radius (r_{in}) approaches zero, a^2r^2 is comparable to r_{in} and, therefore, Eq. 35 should be used. In this work, because we took the radius, $\phi = 0$, for which $r_{in} = 0$, we used Eq. 35 to calculate the average radial thermal conductivity. If, for example, the radius $\phi = \pi$ or 2π were picked, then r_{in} would be sufficiently large and either one of Eq. 35 and 40 could be used.

The 1D-radial model (*i.e.*, Eq. 7-11) is the same in form as the 1D-radial-spiral model (*i.e.*, Eq. 30-34) except that in the latter model both radial and spiral heat conductions are captured through the use of a position dependent effective thermal conductivity given by Eq. 31.

Results and Discussion

The magnitude of the quantity $1/4\pi^2N^2(\lambda_1/\lambda_2)$ determines the importance of spiral heat conduction and, therefore, spiral conduction dominated when the spiral had few winds or was made of materials with very different thermal conductivities. On the other hand, if the spiral had many winds or was made of similar conducting materials, radial heat conduction dominated. These effects are shown in Fig. 3 using the steady-state temperature distributions and heat flow patterns obtained by solving the rigorous 2D model under three different conditions. In the first case (*i.e.*, Fig. 3a) the spiral composite had five winds with the thermal conductivity of the first region being 1000 times smaller than the second, resulting in $1/4\pi^2N^2(\lambda_1/\lambda_2) \approx 1$. Therefore, heat flow was predominantly in the spiral direction in the second region; radial heat flow was impeded by the first region. On the other hand, if the thermal conductivities of the two regions are comparable, heat flow is predominantly radial. This is the second case, shown in Fig. 3b, where the thermal conductivities of the two regions are equal (*i.e.*, $1/4\pi^2N^2(\lambda_1/\lambda_2) \approx 10^{-3}$). When the number of winds was high, heat flow was again predominantly radial even when the thermal conductivities were very different. This case is shown in Fig. 3c, where the thermal conductivity of the first region was 100 times smaller than the second, and the number of winds was 20 (*i.e.*, $1/4\pi^2N^2(\lambda_1/\lambda_2) \approx 6 \times 10^{-3}$).

In all the three cases, the heat-transfer coefficient (h) was set at 100 W/m^2/K, and the heat generation rate ($\dot{q}$) was set at 10^5 W/m^3, a value typically observed in battery systems.[3-10] Changing the value of the heat-transfer coefficient or the heat generation rate changed the local temperatures attained by the battery, but did not change the heat flow pattern. Further, in all the three cases, the rate of change of temperature in the spiral direction was much smaller than in the radial direction. Consequently, any radius of the spiral can be picked for the 1-D models. As mentioned earlier, we chose the radius shown dotted in Fig. 1.

When radial heat conduction dominates, the 1D-radial model should predict temperatures well, while it should show significant errors when spiral heat conduction was important. Thus, by comparing the 1D-radial and the 2D model predictions over a wide range of N and λ_1/λ_2, we identified in Fig. 4 situations when spiral heat conduction was important. The temperature at the center, which was the hottest spot in the spiral, was taken to be the criterion for comparison because an important application of thermal battery models is predicting the hotspots. The outer edge of the spiral is always the coldest as heat generated inside the spiral is lost to the ambience through the outer edge. Further, a very high value of the heat-transfer coefficient (h) is used, which means that the outer temperature of the battery is fixed at the ambient value. Above the solid line given by $1/4\pi^2N^2(\lambda_1/\lambda_2) = 0.1$, the relative error in the 1D-radial model is less than 10% and, therefore, spiral conduction is deemed negligible. For greater values of N or λ_1/λ_2, the 1D-radial model can be used in preference to the 2D model. On the other hand, for smaller values of N or λ_1/λ_2, spiral conduction becomes important and the relative error in the 1D-radial model is greater than 10%.

While the 1D-radial model failed under conditions when spiral conduction was important (*i.e.*, when $1/4\pi^2N^2(\lambda_1/\lambda_2) > 0.1$) we compared the predictions of the 1D-radial-spiral model with the 2-D model. We found that the relative error in the 1D-radial-spiral model was less than 10%, which means that this 1-D model can be used in preference to the 2D model to predict temperatures accurately when spiral conduction is important. However, in the region below the dashed line given by $1/4\pi^2N^2(\lambda_1/\lambda_2) = 10$, the error in the 1D-radial-spiral model became more than 10%. This means that for very small values of N or λ_1/λ_2, the 2-D model must be used to predict temperatures accurately.

Also shown in the figure are approximate positions of some of the spirally wound battery systems considered in the literature.[3-7] Thus, for the lead-Acid, Zn-MnO_2, Li-BCX, and Li-$SOCl_2$ systems spiral heat conduction is important and this is why the authors used the 2D model. However, because all these battery systems fell in the region $0.1 < 1/4\pi^2N^2(\lambda_1/\lambda_2) < 10$, where the 1D-radial-spiral model worked well, it can be used instead of the 2D model. On the other hand, spirally wound Li-ion batteries have a large number of winds (even an 18650-type battery has about 20 winds[2]) making spiral heat conduction negligible. Consequently, the 1D-radial model can be used as was done by Al Hallaj *et al.*[7]

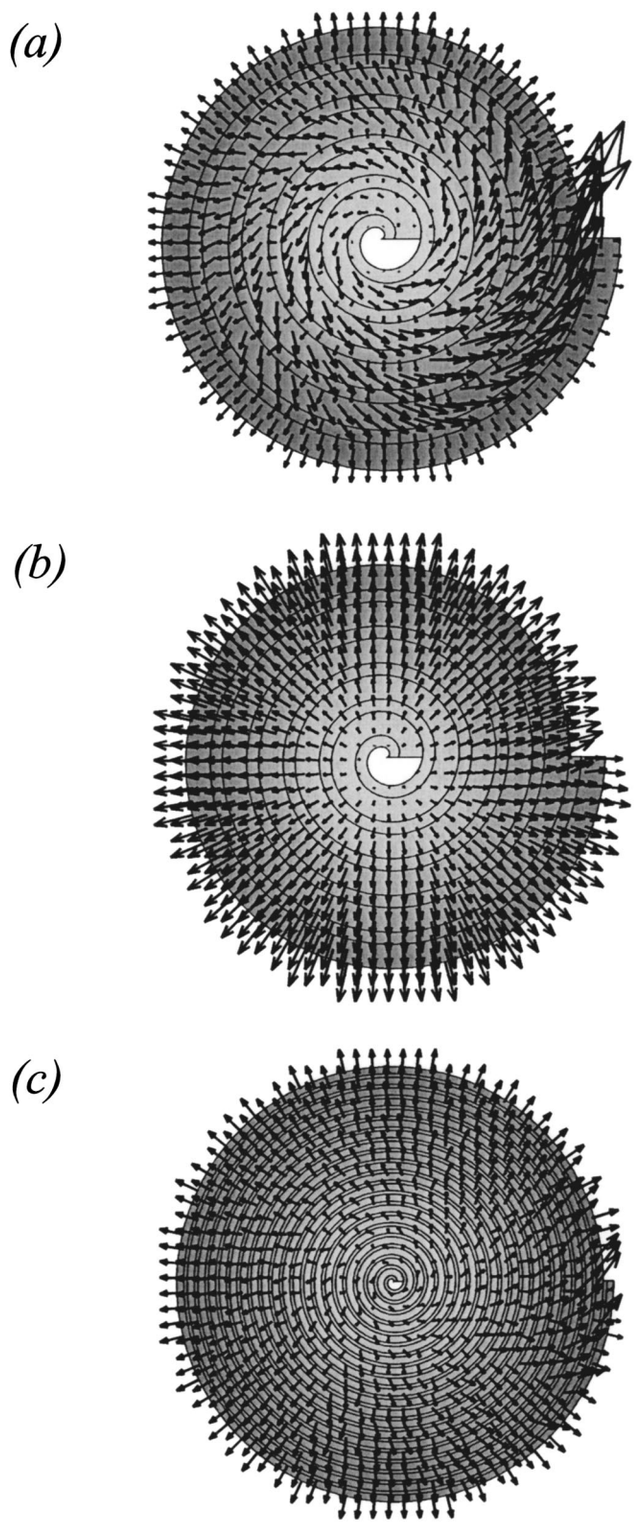

Figure 3. Steady-state temperature distributions and heat flow patterns obtained by solving the rigorous 2D model for (*a*) $N = 5$ and $\lambda_1/\lambda_2 = 10^{-3}$, (*b*) $N = 5$ and $\lambda_1/\lambda_2 = 1$, and (*c*) $N = 20$ and $\lambda_1/\lambda_2 = 10^{-2}$. Darker regions are colder.

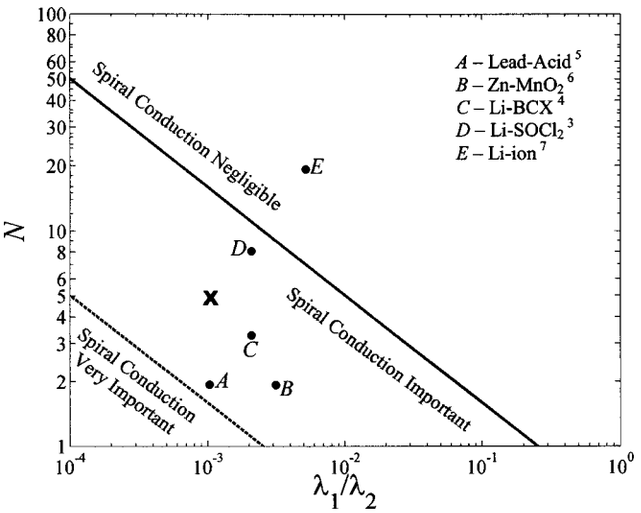

Figure 4. A plot showing regions where spiral conduction is important. The solid and dashed lines correspond to values of 0.1 and 10, respectively, for the quantity $1/4\pi^2 N^2(\lambda_1/\lambda_2)$. Above and below the solid line, the relative error in the 1D-radial model are, respectively, less and greater than 10%. Above and below the dashed line, the relative error in the 1D-radial-spiral model are, respectively, less and greater than 10%. Also shown in the plot are approximate positions of the various spirally wound battery systems considered in the literature. The temperature profiles shown in Fig. 5 are for the point marked **x**.

Example comparisons between the dimensionless temperature profiles predicted by the three models are shown in Fig. 5. The values chosen for N and λ_1/λ_2 correspond to the point marked x in Fig. 4, where spiral conduction was important. Further, parameter values (see Table I) typical of battery systems are used. Four different values were considered for the heat-transfer coefficient (h) representing four different physical situations: (a) $h \to \infty$, when outer temperature is fixed at the ambient value, (b) $h = 100$ W/m^2/K, representing forced convection, (c) $h = 10$ W/m^2/K, representing natural convection, and (*d*) $h = 0$, representing adiabatic operation.

In the first two situations, the 1D-radial-spiral model predicted center temperature better than the 1D-radial model. In the last two situations, all the models agreed because minimal or no heat flow existed when the spiral operated adiabatically. Note that no steady-state existed when $h = 0$, while temperatures unrealistically high for battery systems were required to attain steady-state when $h = 10$ W/m^2/K. Therefore, for these two cases, profiles at the end of 100 time constants (*i.e.*, at $t = 100\tau$) are shown. As mentioned earlier, the temperature profiles were step-like for the discrete models (1D-radial and 2D) because of the alternating thermal conductivities encountered as one moves along a radius. For the 1D-radial-spiral model, however, the temperature profiles were smooth because average thermal properties were used.

The advantage of using the 1-D models over the 2D model is the savings in computational time and in the computer memory required. For example, on a PC Workstation with a 1 GHz Intel Pentium-III processor and a 2 GB RDRAM, the 1D-radial-spiral model took approximately 0.0165 s for a steady-state simulation, while the 2D model took 0.845 s. Even though the 1D-radial-spiral model ran about 50 times faster than the 2-D, both the solution times were small when solving only the energy balance. However, when electrochemistry was coupled to the energy balance, the solution times for simulating a complete 2C discharge were about 20 min with the 1D-radial-spiral model and approximately 20 h with the 2-D model. (The electrochemical models used were those presented in Ref. 14 and 15, respectively, for a Li-ion battery.) Further, if the temperature variation along the battery height is also sought, then

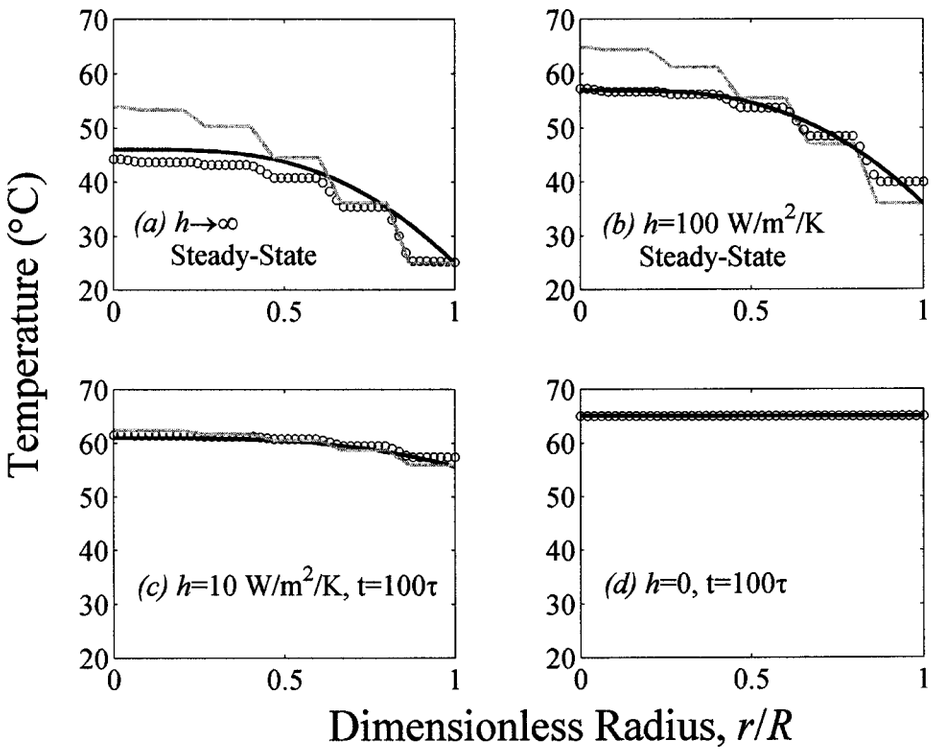

Figure 5. Radial temperature profiles predicted by the three models for the point marked **x** in Fig. 4, where spiral conduction is important. For high values of h, the (black line) 1D-radial-spiral model predicts temperatures much better than the (gray line) 1D-radial model, while under adiabatic conditions all the models agree exactly. (open circles) The predictions of the rigorous 2D model are shown.

the 3-D temperature distribution required can be obtained by solving just a 2-D (radial and axial) model, reducing solution time by several days.

Conclusion

A general method is presented by which the 2-D problem (the 2D model) of heat conduction in a spiral geometry was reduced to a 1-D problem (the 1D-radial-spiral model) through a coordinate transformation approach. The 1D-radial-spiral model treated the spiral composite as a single homogeneous region with average thermal properties. Even though 1-D, the 1D-radial-spiral model captured both radial and spiral heat conductions through a position-dependent effective thermal conductivity. The effective thermal conductivity is a combination of average radial and spiral thermal conductivities. While the thermal conductivity of the more conductive region was used as the average spiral thermal conductivity, the discrete form of the governing equation was integrated to obtain an expression for the average radial thermal conductivity.

The 1D-radial model worked well either when operated close to adiabatic conditions or when spiral conduction was negligible; when spiral conduction became important, the 1D-radial model did not predict temperatures adequately.

Significant spiral heat conduction is encountered in many battery systems having few winds and wherein the current collector has a much larger thermal conductivity than the separator. Under these conditions, the 1D-radial-spiral model predicts temperatures adequately and can, therefore, be used in preference to the 2D model. By doing so computational time is reduced from approximately 20 h to 20 min when solving a coupled electrochemical-thermal model.

Table I. List of Parameter Values.

Parameter	Value
$\dot{q}$	10^5 W/m^3
R	20 mm
λ_1	0.1 W/m/K
λ_2	100 W/m/K
N	5

Acknowledgment

The authors acknowledge the *National Reconnaissance Office* for funding this research under contract no. 1999 I016400 000 000.

The University of South Carolina assisted in meeting the publication costs of this article.

List of Symbols

a	as defined in Eq. 13
A/V	surface area-to-volume ratio
A_1, A_2	areas occupied by the materials S_1 and S_2 (see Eq. 29)
C_p	specific heat capacity
h	heat-transfer coefficient
h'	modified heat-transfer coefficient as defined in Eq. 15
l	spiral coordinate
N	number of winds in the spiral
$\dot{q}$	local heat generation rate
Q	heat flux
r	radial coordinate
r_0	distance of the center of the spiral composite from the origin ($r_0 = 0$ here)
r_A, r_B	as defined in Eq. 36-39
r_{in}	inner radius of the spiral
R	ring-thickness of a spiral (see Fig. 1)
S_1, S_2	component materials of the spiral composite (see Fig. 1)
t	time
T	temperature
x, y	rectangular Cartesian coordinates
X, X_0	as defined in Fig. 2
X_1, X_2	thicknesses of the materials S_1 and S_2 (see Fig. 1)

Greek

θ, ϕ	angular coordinates
λ	thermal conductivity
ρ	density
τ	time constant, $\rho C_p\|_{eff} R^2/\lambda_{eff}$

Subscripts

0	initial

1 region 1
2 region 2
∞ steady state
amb ambient
eff effective
l spiral component
r radial component

References

1. R. G. Gruenstern and J. R. Pierson, *J. Power Sources*, **91**, 62 (2000).
2. R. Spotnitz, *Advances in Lithium-Ion Batteries*, W. A. van Schalkwijk and B. Scrosati, Editors, p. 433, Kluwer Academic/Plenum Publishers, New York (2002).
3. T. I. Evans and R. E. White, *J. Electrochem. Soc.*, **136**, 2145 (1989).
4. E. E. Kalu and R. E. White, *J. Electrochem. Soc.*, **140**, 23 (1993).
5. J. N. Harb and R. M. LaFollette, *J. Electrochem. Soc.*, **146**, 809 (1999).
6. E. J. Podlaha and H. Y. Cheh, *J. Electrochem. Soc.*, **141**, 1751 (1994).
7. S. Al Hallaj, H. Maleki, J. S. Hong, and J. R. Selman, *J. Power Sources*, **83**, 1 (1999).
8. Y. I. Cho and G. Halpert, *J. Power Sources*, **18**, 109 (1986).
9. Y. I. Cho, *J. Electrochem. Soc.*, **134**, 771 (1987).
10. L. Rao and J. Newman, *J. Electrochem. Soc.*, **144**, 2697 (1997).
11. L. Song and J. W. Evans, *J. Electrochem. Soc.*, **147**, 2086 (2000).
12. J. Wu, V. Srinivasan, J. Xu, and C. Y. Wang, *J. Electrochem. Soc.*, **149**, A1342 (2002).
13. R. B. Bird, W. E. Stewart, and E. N. Lightfoot, *Transport Phenomena*, John Wiley & Sons, New York (2002).
14. P. M. Gomadam, R. E. White, and J. W. Weidner, *J. Electrochem. Soc.*, Submitted.
15. P. M. Gomadam, J. W. Weidner, R. A. Dougal, and R. E. White, *J. Power Sources*, **110**, 267 (2002).